Combustion and Flame 269 (2024) 113698

Contents lists available at ScienceDirect

Combustion and Flame

journal homepage: www.sciencedirect.com/journal/combustion-and-flame

Systematically derived reduced kinetics for hydrogen/ammonia gas-turbine combustion

Brandon Li [a,*], Daniel Fernández-Galisteo [b], Antonio L. Sánchez [a], Forman A. Williams [a]

[a] Dept. Mechanical and Aerospace Engineering, University of California San Diego, La Jolla CA 92093-0411, USA
[b] Department of Energy, Centro de Investigaciones Energéticas, Medioambientales y Tecnológicas, Madrid, 28040, Spain

ARTICLE INFO

Keywords:
Hydrogen-ammonia oxidation
Reduced chemical kinetics
Gas-turbine combustion

ABSTRACT

Starting with a detailed-chemistry description involving 20 elementary steps for hydrogen oxidation and 40 elementary steps for ammonia oxidation, it is shown that systematic application of sensitivity analyses of premixed flames under typical gas-turbine combustion conditions reduces the description to 12 elementary steps for hydrogen oxidation, 4 of them being reversible, and an additional 19 steps for ammonia oxidation, 6 of them being reversible, yielding reasonable predictions for auto-ignition and deflagration processes. Subsequent introduction of steady-state approximations for chemical intermediates, afforded by the high-pressure conditions existing in gas-turbine combustion chambers, effectively reduces the fuel-oxidation description in systems utilizing H_2-NH_3 fuel mixtures to two global steps for deflagrations, namely, $2H_2 + O_2 \rightleftharpoons 2H_2O$ and $4NH_3 + 3O_2 \rightleftharpoons 2N_2 + 6H_2O$. Analytical expressions for the associated overall rates, involving the local temperature and the O_2, H_2, NH_3, N_2, and H_2O concentrations, are derived through selective truncation of the steady-state expressions, resulting in a simplified chemistry description that can facilitate future numerical analyses based on direct-numerical and large-eddy simulations.

Novelty and significance statement

A new short mechanism involving only 31 elementary reactions between 16 reactive species has been derived for hydrogen-ammonia oxidation under conditions of pressure, temperature and dilution typically found in gas-turbine burners. Introduction of steady-state assumptions for all intermediate species leads to a two-step mechanism that is shown to predict burning rates with sufficient accuracy. The proposed mechanism can significantly reduce computational times in future direct-numerical and large-eddy simulations.

1. Introduction

The continued necessity of large-scale on-demand power generation and propulsion, in the face of mushrooming environmental needs for reducing emissions of carbon dioxide and dependence on fossil fuels, focuses attention on gas turbines as essential components of any system [1]. This has generated thorough investigations of reduction techniques, including both pre-combustion and post-combustion carbon capture and sequestration [2]. Manufacturers are moving from systems fueled by natural gas to new designs involving alternative fuels, such as hydrogen, to support carbon-free energy-production [3]. The high reactivity of hydrogen can necessitate substantial modifications in designs of gas-turbine combustion chambers [4]. Mixtures of hydrogen with ammonia, however, exhibit burning velocities closer to those of natural gas, making them attractive alternatives [5]. Ammonia addition also can be helpful in enhancing safety of hydrogen transport through transmission lines, and its low storage cost and mature production methods make it a promising candidate for employment in alternative fuels. A critical need therefore exists for simple and efficient means for describing the chemical kinetics of hydrogen-ammonia combustion under gas-turbine conditions. The use of detailed-chemistry descriptions in numerical simulations at high Reynolds numbers or in complex configurations excessively taxes computational capabilities, thereby motivating the present analysis, focused on the development of a systematically reduced chemical-kinetic description for H_2-NH_3 oxidation that has sufficient accuracy to yield reliable computational results.

Thorough up-to-date reviews of research on detailed and reduced chemical-kinetic mechanisms for the oxidation of ammonia and hydrogen are available in the literature [6–10]. We would call the reader's attention to [6,10] for especially informative discussions. Since there seems to be no reason to repeat those discussions here, this very extensive work is not cited in the present introduction. While these previous studies addressed both detailed and reduced mechanisms (emphasizing

* Corresponding author.
E-mail address: bwl003@ucsd.edu (B. Li).

https://doi.org/10.1016/j.combustflame.2024.113698
Received 15 April 2024; Received in revised form 23 August 2024; Accepted 23 August 2024
Available online 5 September 2024

the important computational benefits of mechanism reduction [6]), with few notable exceptions, such as [11], even the shortest reduced mechanisms previously considered are appreciably longer than the short mechanism considered herein for beginning our reduction. We thus focus on the possibilities of developing greater reductions to achieve further computational convenience for the decreased ranges of conditions expected in foreseeable gas-turbine applications. Consistent with that objective, we shall not address NOx production, presuming that flame temperatures are to be kept low enough to reduce such problems, nor shall we consider pure hydrogen without ammonia addition, which has been analyzed similarly in previous work by us and others [12]. The pioneering work of Lindstedt and Selim [11] on ammonia-oxygen chemistry identified mechanisms as short as four steps, through methods of the same type that are to be employed herein. Their results, however, are quite different from ours, since they apply at lower pressures and higher temperatures than will be considered here. The results to be derived below may be considered to have been obtained by employing the methods of Lindstedt and Selim to the higher-pressure conditions that pertain to present-day and future gas turbines in which chamber temperatures are purposely kept low enough to prevent excessive NOx formation.

2. A short mechanism for H_2/NH_3 oxidation

The chemistry reduction starts from a detailed mechanism developed recently [5], which includes 20 hydrogen steps from the San Diego mechanism [13] along with 40 ammonia steps, developed by adding 6 additional steps and a new reactive species (H_2NO) to the original nitrogen-chemistry component of San Diego mechanism. The predictive accuracy of the resulting 60-step scheme has been tested through comparisons with experimental measurements of ignition delay times, laminar velocities of freely propagating deflagrations, extinction strain rates of counterflow back-to-back premixed flames, and NO profiles in burner-stabilized flat flames [5]. Sample comparisons, additional to those presented earlier in [5], are given in Fig. 1, where the symbols represent experimental measurements of flame propagation velocities (upper plot) and ignition delay times (lower plot), while the curves are results of numerical calculations. The flames are computed with a multicomponent transport description including thermal diffusion [14,15], while the ignition time is determined in constant-pressure homogeneous computations using peak H-atom concentrations to identify ignition. As can be seen, although there is some variance in the experimentally measured flame speeds [16,17], the detailed mechanism, represented with a solid curve, correctly predicts the increase in burning rate with increasing hydrogen content. Similarly, the ignition delay computed numerically compares well with the values measured in rapid-compression-machine experiments [18].

A systematic sensitivity analysis based on computations of one-dimensional steady $H_2/NH_3/N_2/O_2$ deflagrations was performed to identify and eliminate elementary chemical reactions and intermediate species that contribute negligibly to the overall fuel-oxidation process under conditions of pressure, temperature and dilution typically found in gas-turbine combustors. Specifically, the study considered combustion at 20 and 40 atmospheres with an upstream temperature of T_u = 700 K over a wide range of equivalence ratios

$$\phi = \frac{3r+2}{4(r+1)}\frac{X_{H_2}+X_{NH_3}}{X_{O_2}}, \tag{1}$$

with $r = X_{NH_3}/X_{H_2}$ representing the ammonia-to-hydrogen mole-fraction ratio. The computations presented below correspond to four different fuel mixtures, including pure ammonia, for which (1) takes the limiting form $\phi = 3X_{NH_3}/(4X_{O_2})$, along with 25%–75%, 50%–50% and 75%–25% hydrogen-ammonia fuel mixtures. To approximate effects of exhaust-gas recirculation, commonly used in gas turbines to lower the adiabatic flame temperature, the mixture is diluted with extra nitrogen. The nitrogen-to-oxygen mole-fraction ratio selected in the computations X_{N_2}/X_{O_2} = 5.515, larger than that of air $X_{N_2}/X_{O_2} \simeq 3.76$, is chosen so that the adiabatic temperature of the stoichiometric flame is approximately 2200 K, as needed to keep emissions of thermal NOx manageable.

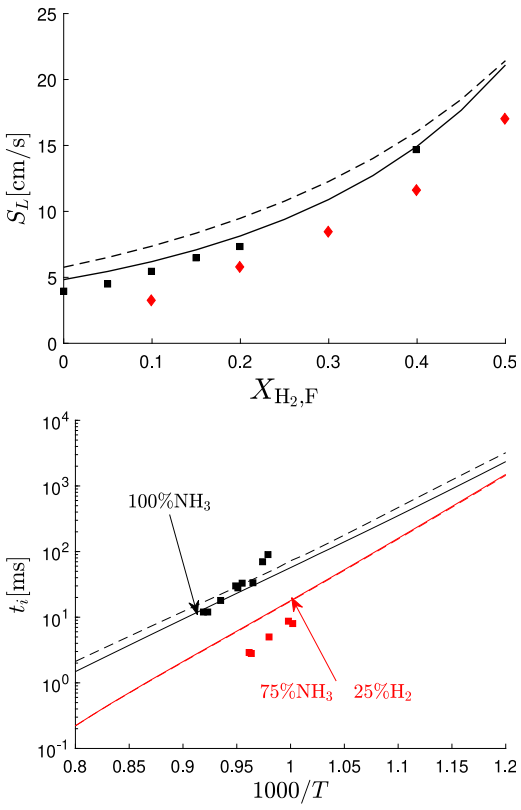

Fig. 1. The upper plot compares the variation with the mole fraction of hydrogen in the fuel mixture $X_{H_2,F}$ of the laminar burning rate S_L computed numerically with the detailed chemistry (solid curve) and short chemistry (dashed curve) with that determined experimentally ([16]: black squares; [17]: red diamonds) for an H_2/NH_3-Air stoichiometric mixture at pressure p = 4.9 atm and temperature T = 298 K. The lower plot compares ignition delay times t_i at p = 42.8 atmospheres as obtained from numerical integrations with detailed (solid curves) and short (dashed curves) chemistry, and from rapid-compression-machine measurements [18], using maximum rate of pressure rise to identify ignition, for NH_3-air (black) and NH_3-H_2-air (75%–25%, red) mixtures with equivalence ratio ϕ = 0.35. (For interpretation of the references to color in this figure legend, the reader is referred to the web version of this article.)

The analysis revealed that only 12 of the starting 20 elementary steps describing H_2 oxidation need to be considered in describing deflagrations, in agreement with previous results pertaining to pure hydrogen [12]. These 12 reactions are listed in Table 1, along with their corresponding reaction-rate parameters. Backward rates are unimportant for most reactions, the only exceptions being the shuffle reactions 1–3, whose backward rates moderate the radical-pool composition, and the hydroperoxyl-consumption step 6, whose backward rate, although entirely unimportant for flame propagation [12], is key in enabling autoignition processes [19]. Regarding the nitrogen chemistry, it was found that N, N_2O, and NO_2 do not play a major role in the fuel-oxidation process and can be correspondingly removed from the mechanism – along with their associated elementary reactions – without deteriorating burning-rate predictions. Additional elimination of a number of elementary reactions, motivated by their negligibly small associated rates, led to the subset of 19 steps for nitrogen oxidation listed in Table 1, 6 of them being reversible.

The predictive capability of the short mechanism is illustrated in Fig. 1, where corresponding results are represented by dashed curves. As can be seen, the comparison of the flame speed predicted with the short mechanism with the detailed-chemistry results indicates that the

Table 1
Rate coefficients in Arrhenius form $k = AT^n \exp(-T_a/T)$ for the 31 steps of the short mechanism with rate parameters in mol, s, cm^3, and K (the sum of two Arrhenius terms is employed to represent the complex temperature dependence of the rate constants of reactions $7f$ and $11f$). The nonunity Chaperon efficiency factors in reaction $4f$ are $\epsilon_{H_2} = 2.5$ and $\epsilon_{H_2O} = 16$ with Troe falloff $F_c = 0.5$, while $\epsilon_{H_2} = 2.5$, $\epsilon_{H_2O} = 6$ and $\epsilon_{H_2O_2} = 6$ in reaction $10f$ and $\epsilon_{H_2O} = 5$ in reaction 28.

Reaction		A	n	T_a
1. $H + O_2 \rightleftharpoons OH + O$		3.52×10^{16}	−0.7	8590
2. $H_2 + O \rightleftharpoons OH + H$		5.06×10^{4}	2.7	3165
3. $H_2 + OH \rightleftharpoons H_2O + H$		1.17×10^{9}	1.3	1829
4f. $H + O_2 + M \rightarrow HO_2 + M$	k_∞	4.65×10^{12}	0.44	0
	k_0	5.75×10^{19}	−1.4	0
5f. $HO_2 + H \rightarrow OH + OH$		7.08×10^{13}	0	148
6. $HO_2 + H \rightleftharpoons H_2 + O_2$		1.66×10^{13}	0	414
7f. $HO_2 + OH \rightarrow H_2O + O_2$		7×10^{12}	0	−550.9
		4.5×10^{14}	0	5500
8f. $H + OH + M \rightarrow H_2O + M$		4×10^{22}	−2	0
9f. $H + H + M \rightarrow H_2 + M$		1.3×10^{18}	−1	0
10f. $H_2O_2 + M \rightarrow OH + OH + M$	k_∞	2.63×10^{19}	−1.3	25 704
	k_0	7.6×10^{30}	−4.2	25 704
11f. $HO_2 + HO_2 \rightarrow H_2O_2 + O_2$		1.03×10^{14}	0	5557
		1.94×10^{11}	0	−709
12f. $HO_2 + H_2 \rightarrow H_2O_2 + H$		7.8×10^{10}	0.6	12 046
13f. $NH + OH \rightarrow HNO + H$		4.0×10^{13}	0	0
14f. $NH + O_2 \rightarrow HNO + O$		4.6×10^{5}	2	3272
15f. $NH + NO \rightarrow N_2 + OH$		2.2×10^{13}	−0.2	0
16. $NH_2 + H \rightleftharpoons NH + H_2$		4×10^{13}	0	1838
17f. $NH_2 + O \rightarrow HNO + H$		6.6×10^{14}	−0.5	0
18f. $NH_2 + O_2 \rightarrow H_2NO + O$		2.6×10^{11}	0.5	14 619
19f. $NH_2 + OH \rightarrow NH + H_2O$		4×10^{6}	2	504
20f. $NH_2 + NO \rightarrow N_2 + H_2O$		2.8×10^{20}	−2.7	633
21f. $NH_2 + NO \rightarrow N_2H + OH$		3.1×10^{13}	−0.5	594
22. $NH_3 + M \rightleftharpoons NH_2 + H + M$		2.2×10^{16}	0	47 029
23. $NH_3 + H \rightleftharpoons NH_2 + H_2$		6.4×10^{5}	2.4	5124
24f. $NH_3 + O \rightarrow NH_2 + OH$		9.4×10^{6}	1.9	3254
25. $NH_3 + OH \rightleftharpoons NH_2 + H_2O$		2.04×10^{6}	2	285
26f. $N_2H + O_2 \rightarrow N_2 + HO_2$		2×10^{14}	0	0
27. $N_2H + M \rightleftharpoons N_2 + H + M$	k_∞	6.5×10^{7}	0	0
	k_0	5×10^{13}	0	0
28. $H + NO + M \rightleftharpoons HNO + M$	k_∞	1.5×10^{15}	−0.4	0
	k_0	4.3×10^{14}	0.206	−783
29f. $HNO + H \rightarrow NO + H_2$		4.4×10^{11}	0.7	327
30f. $HNO + OH \rightarrow NO + H_2O$		3.6×10^{13}	0	0
31f. $H_2NO + HO_2 \rightarrow HNO + H_2O_2$		2.9×10^{4}	2.7	−805

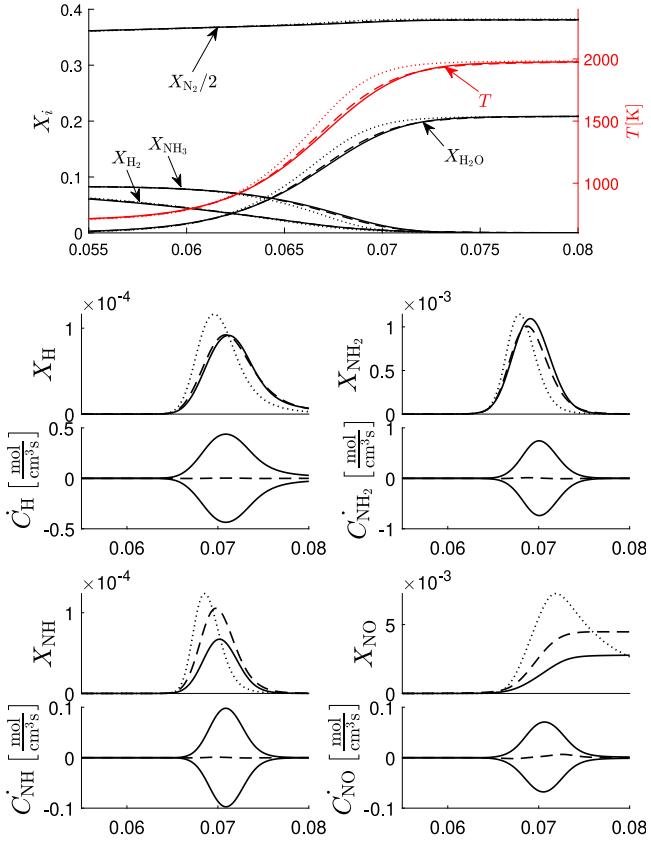

Fig. 2. Temperature and mole-fraction distributions of main species and selected intermediates (H, NH_2, NH, and NO) across a 50%–50% H_2-NH_3 lean flame with $\phi = 0.8$ and $X_{N_2}/X_{O_2} = 5.515$ as obtained numerically (solid curves: detailed chemistry; dashed curves: short chemistry; dotted curves: two-step reduced mechanism) for an initial temperature $T_u = 700$ K and a pressure $p = 20$ atmospheres. For each chemical intermediate, the corresponding bottom panel shows the distributions of production and consumption rates (solid curves) and transport rates (dashed curves) found in the detailed-chemistry computations.

differences between both descriptions are on the order of variances observed between different experimental data. It is also noteworthy that, although the development of the short mechanism was based on laminar-deflagration computations, the mechanism retains its predictive capability regarding autoignition processes, as can be seen by the comparisons shown in the lower plot of the figure.

To further illustrate the level of accuracy of the short mechanism, Fig. 2 compares temperature and reactant mole-fraction profiles, along with mole-fraction profiles of radicals representative of the hydrogen and nitrogen reactant pools, for a condition illustrative of those of interest. It can be seen from this figure that the agreement is excellent, the largest difference, on the order of a factor of two, appearing in the NH and NO profiles. These differences, including the overprediction in the NO equilibrium value, which do not affect the predictive capability of the short mechanism regarding burning rates, suggest that additional elementary reactions must be included in the short mechanism to enable accurate computations of NO production.

Results of predictions of laminar burning rates are shown in Fig. 3 for various fuel mixtures and two different pressures. The departures between the detailed-chemistry results, represented by solid curves, and the short-chemistry results, represented by dashed curves, are typically smaller than 5% over the whole range of flammability conditions (dotted and dot-dashed curves, corresponding to results of the two-step chemistry, are to be discussed later). The curves are practically indistinguishable for the 50%–50% H_2-NH_3 mixture, an attractive fuel replacement in retrofit efforts involving natural-gas systems, since the resulting burning rates are comparable to those of methane. For the fuel mixtures with significant ammonia content, the curves display a pronounced increase in slope as the equivalence ratio rises above $\phi \simeq 0.9-1$, a feature of high-pressure ammonia combustion captured in previous computations (see, e.g., the results shown in Fig. 5c of [20]). Because of the reduction in the number of chemical species and elementary reactions, the computations using the short chemistry were found to be about 30% faster than those using detailed chemistry.

The performance of the short mechanism in connection with strained flamelets was investigated in computations of twin premixed flames in axisymmetric counterflow mixing layers at $p = 40$ atm, with results shown in Fig. 4. The opposed streams contain a preheated lean mixture of H_2, NH_3, N_2, and O_2 with $\phi = 0.6$ and $T = 700$ K. The plots represent the variation of the peak temperature over a wide range of strain rates A for three different fuel compositions, with $X_{N_2}/X_{O_2} = 5.515$ in all cases, as is consistent with the premixed unstrained deflagrations shown earlier in Fig. 3. In the computations, the value of A was increased until extinction was observed at a given critical value, higher for higher hydrogen content. This increased burning capability is consistent with the flame-speed results of Fig. 3. The curves show the expected superadiabatic temperature associated with preferential diffusion effects [21], more pronounced for fuel mixtures with a higher hydrogen content. The comparison of the results of the detailed chemistry (solid curves) with those of the short chemistry (dashed curves) reveals that the latter mechanism predicts with sufficient accuracy the flame response to stretch, including the critical value of the strain rate at extinction.

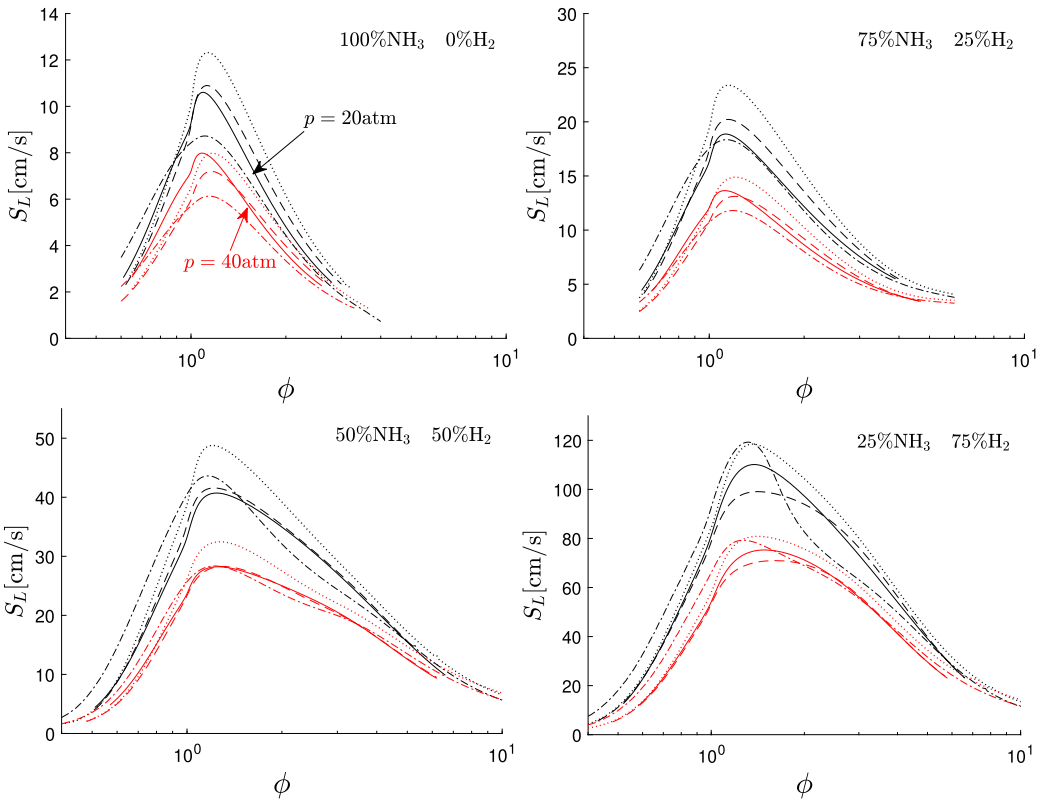

Fig. 3. The variation with equivalence ratio of the laminar burning rate S_L of $NH_3/H_2/N_2/O_2$ mixtures with $X_{N_2}/X_{O_2} = 5.515$ and $T_u = 700$ K as obtained numerically using the 60-step detailed mechanism (solid curves), the 31-step short mechanism (dashed curves), the two-step reduced mechanism (dotted curves) and the two-step mechanism with truncated steady-state expressions (dot-dashed curves) for $p = 20$ atmospheres (black) and $p = 40$ atmospheres (red). (For interpretation of the references to color in this figure legend, the reader is referred to the web version of this article.)

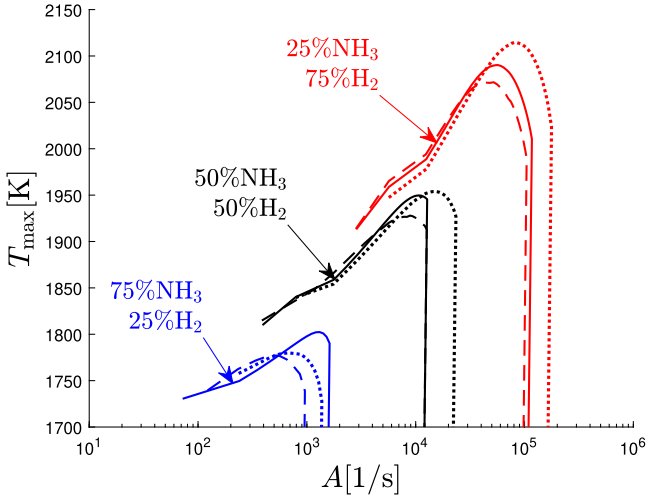

Fig. 4. The variation with strain rate A of the peak temperature of twin premixed flames in axisymmetric counterflows of opposed streams of H_2, NH_3, N_2, and O_2 with $\phi = 0.6$, $X_{N_2}/X_{O_2} = 5.515$, and $T = 700$ K at $p = 40$ atm as obtained numerically using the 60-step detailed mechanism (solid curves), the 31-step short mechanism (thin solid curves), and the two-step reduced mechanism (dotted curves).

3. The two-step reduced mechanism

Additional simplification can be achieved through introduction of steady-state approximations for chemical intermediates that exhibit transport rates that are small compared with their corresponding production and consumption rates [22], so that in the first approximation one can replace the species transport equation (a partial differential equation) with an algebraic equation expressing the local production–consumption balance [23]. For ammonia oxidation, this kind of approach has been shown to produce reduced mechanisms that provide reasonable accuracy in computations of laminar deflagrations at ambient pressure [11]. The simplest previously available description involved four overall reactions, with NO and H as the only intermediates not following a steady-state approximation. The present analysis focuses on high-pressure combustion at temperatures low enough to avoid appreciable thermal NO production, for which the steady-state approximation will be seen to apply to these two intermediaries as well, with accuracy sufficient for predicting overall rates, thereby reducing the description to two global reactions involving only the reactants (H_2, NH_3 and O_2) and the main products (N_2, H_2O). Similar ideas have been recently applied to the description of high-pressure hydrogen oxidation, resulting in a simple one-step reaction with an explicit rate expression [24].

To illustrate the applicability of the steady-state approximation for H_2/NH_3 combustion at high pressure, Fig. 2 includes four panels showing the variation across the flame of the rates of production, consumption, and transport of H, NH_2, NH, and NO. As can be seen, in all cases the transport rate is everywhere much smaller than the chemical rates. Similar steady-state agreements apply also for O, OH, HO_2, H_2O_2, N_2H, HNO, and H_2NO, not shown in the figure. From these results it can be concluded that for eleven of the sixteen species present in the short mechanism of Table 1 transport equations can be replaced by the steady-state algebraic equations resulting from the local balance between consumption and production. The associated balance equations are listed for convenience in Table 2, where ω_i denotes the rate of elementary reaction i (mols per unit volume per unit time). With five species remaining in the description, application of atom

Table 2
The steady-state equations involved in the derivation of the two-step reduced chemistry. The terms in bold remain after truncations.

H_2NO	$\boldsymbol{\omega_{31f} = \omega_{18f}}$
NH_2	$\boldsymbol{\omega_{16f}} + \omega_{17f} + \boldsymbol{\omega_{18f}} + \omega_{19f} + \omega_{20f} + \omega_{21f} + \boldsymbol{\omega_{22b}} + \boldsymbol{\omega_{23b}} + \boldsymbol{\omega_{25b}} =$ $\omega_{16b} + \boldsymbol{\omega_{22f}} + \boldsymbol{\omega_{23f}} + \boldsymbol{\omega_{24f}} + \boldsymbol{\omega_{25f}}$
NH	$\boldsymbol{\omega_{13f}} + \boldsymbol{\omega_{14f}} + \omega_{15f} + \boldsymbol{\omega_{16b}} = \boldsymbol{\omega_{16f}} + \boldsymbol{\omega_{19f}}$
HNO	$\boldsymbol{\omega_{28b}} + \omega_{29f} + \omega_{30f} = \omega_{13f} + \boldsymbol{\omega_{14f}} + \omega_{17f} + \omega_{28f} + \boldsymbol{\omega_{31f}}$
NO	$\omega_{15f} + \boldsymbol{\omega_{20f}} + \boldsymbol{\omega_{21f}} + \omega_{28f} = \boldsymbol{\omega_{28b}} + \omega_{29f} + \omega_{30f}$
N_2H	$\boldsymbol{\omega_{26f}} + \boldsymbol{\omega_{27f}} = \boldsymbol{\omega_{21f}} + \omega_{27b}$
H	$\boldsymbol{\omega_{1f}} + \omega_{2b} + \boldsymbol{\omega_{3b}} + \boldsymbol{\omega_{4f}} + \boldsymbol{\omega_{5f}} + \boldsymbol{\omega_{6f}} + \omega_{8f} + 2\omega_{9f} + \boldsymbol{\omega_{16f}} + \boldsymbol{\omega_{22b}} + \boldsymbol{\omega_{23f}} + \omega_{27b} + \omega_{28f} + \omega_{29f} =$ $\omega_{1b} + \boldsymbol{\omega_{2f}} + \boldsymbol{\omega_{3f}} + \omega_{6b} + \omega_{12f} + \omega_{13f} + \boldsymbol{\omega_{16b}} + \omega_{17f} + \boldsymbol{\omega_{22f}} + \boldsymbol{\omega_{23b}} + \omega_{27f} + \boldsymbol{\omega_{28b}}$
O	$\omega_{1b} + \boldsymbol{\omega_{2f}} + \omega_{17f} + \boldsymbol{\omega_{24f}} = \boldsymbol{\omega_{1f}} + \omega_{2b} + \omega_{14f} + \boldsymbol{\omega_{18f}}$
OH	$\omega_{1b} + \boldsymbol{\omega_{2b}} + \boldsymbol{\omega_{3f}} + \boldsymbol{\omega_{7f}} + \boldsymbol{\omega_{8f}} + \omega_{13f} + \boldsymbol{\omega_{19f}} + \boldsymbol{\omega_{25f}} + \omega_{30f} =$ $\boldsymbol{\omega_{1f}} + \boldsymbol{\omega_{2f}} + \boldsymbol{\omega_{3b}} + \boldsymbol{2\omega_{5f}} + \boldsymbol{2\omega_{10f}} + \omega_{15f} + \omega_{21f} + \boldsymbol{\omega_{24f}} + \boldsymbol{\omega_{25b}}$
HO_2	$\boldsymbol{\omega_{5f}} + \boldsymbol{\omega_{6f}} + \omega_{7f} + \boldsymbol{2\omega_{11f}} + \boldsymbol{\omega_{12f}} + \omega_{31f} = \boldsymbol{\omega_{4f}} + \omega_{6b} + \omega_{26f}$
H_2O_2	$\boldsymbol{\omega_{10f}} = \boldsymbol{\omega_{11f}} + \boldsymbol{\omega_{12f}} + \omega_{31f}$

conservation effectively reduces the chemistry to two overall steps, which can be conveniently cast in the form

$$2H_2 + O_2 \overset{\text{I}}{\rightleftharpoons} 2H_2O$$
$$4NH_3 + 3O_2 \overset{\text{II}}{\rightleftharpoons} 2N_2 + 6H_2O$$

with overall rates given by

$$\omega_{\text{I}} = \omega_{4f} + \omega_{8f} + \omega_{9f} - \omega_{11f} - \omega_{12f} - \omega_{18f} - \omega_{22} - \omega_{27} + \frac{1}{2}\left(\omega_{28} + \omega_{29f} + \omega_{30f}\right), \tag{2}$$

$$\omega_{\text{II}} = \frac{1}{2}\left(\omega_{15f} + \omega_{20f} + \omega_{21f}\right). \tag{3}$$

Note that the proposed two-step description is not unique, in that any linear combination of the two global reactions could be used to replace one of them. Also, the assigned rates could be expressed as a different combination of elementary reactions by using the steady-state algebraic equations in Table 2. The specific form shown above has been selected to express separately the oxidation of the two fuel components. With this selection, for combustion of pure hydrogen, for which nitrogen chemistry is negligibly slow, one can simply discard the second overall reaction, and write the overall hydrogen-oxidation rate in the form $\omega_{\text{I}} = \omega_{4f} + \omega_{8f} + \omega_{9f} - \omega_{11f} - \omega_{12f}$, which further reduces to $\omega_{\text{I}} = \omega_{4f} + \omega_{8f} + \omega_{9f}$ if H_2O_2 is neglected, as was done in our previous one-step reduced mechanism for high-pressure hydrogen combustion [24].

4. Flame computations with the two-step mechanism

Numerical computations using the two-step reduced chemistry involve in general the integration of the transport equations for the five reactive species H_2, NH_3 and O_2, N_2, and H_2O along with the conservation equations of mass, momentum and temperature. The concentration of the eleven steady-state species C_{H}, C_{NH_2}, …, needed to evaluate the overall oxidation rates in Eqs. (3) and (3), can be computed in terms of the concentration of the main species C_{H_2}, C_{NH_3}, … and the temperature T with use of the eleven nonlinear algebraic equations given in Table 2. Because of their complexity, closed-form analytic expressions for the concentrations of the intermediates, which are available for the oxidation of pure hydrogen [24], cannot be easily derived, so that a numerical solver is in general required. For the steady laminar flames computed with the reduced mechanism, a Newton method was implemented for the solution at a given grid point, with extrapolation of the concentrations at grid points located immediately upstream used to define the initial guess to initialize the iteration. No convergence problems were found with mixtures of hydrogen and ammonia. However, the proposed steady-state equations do exhibit convergence issues with pure hydrogen flames. This is likely due to the inclusion of H_2O_2 which is necessary for the description of hydrogen-ammonia mixtures. For pure hydrogen chemistry, the rates and corresponding elementary reactions must be explicitly reduced to the one-step mechanism for high-pressure hydrogen combustion [24], as discussed previously. In fact, the two-step reduced mechanism converges even with a very small initial mole fraction of ammonia, down to less than 10^{-3}, although with some deviations in the laminar burning velocity from the detailed and short mechanisms for cases with minuscule amounts of ammonia. With the steady-state approximation, the associated computational times were found to be about a factor of 10 smaller than those involved in the corresponding computations using the detailed chemistry.

The accuracy of the two-step description is illustrated in Fig. 2, with dotted curves used to represent the associated numerical results. The reduced kinetics is seen to provide an accurate description of the flame structure, including profiles of temperature and main chemical species across the flame, which are depicted in the upper panel. The results in the bottom panels for different chemical intermediates reveal that the steady-state approximation is sufficiently accurate for the H, NH_2, and NH, the main radicals controlling the fuel-oxidation rate. In contrast, the departures shown by the NO profile indicate that the steady-state approximation results in errors that are much too large, implying that a reduced mechanism with NO out of steady state, involving a minimum of three overall reactions, would be needed for computations of NO emissions.

Burning rates obtained with the two-step mechanism are shown as dotted curves in Fig. 3. Satisfactory results are obtained for the four fuel mixtures considered. The two-step description is particularly accurate in describing the lean and stoichiometric flames prevailing in most practical systems. For fuel mixtures containing ammonia, the steady-state approximations tend to magnify the rapid rise of burning rate occurring as the mixture transitions from lean to rich, leading to predictions of peak velocities that exceed those of the detailed chemistry by about 15%. The performance of the two-step chemistry in describing flames under stretch is tested in Fig. 4. The level of accuracy is seen to be similar to that encountered in the computation of unstrained flames. As can be expected from the introduction of the steady-state approximations, the extinction strain rates of NH_3/H_2-air flames predicted with the two-step mechanism are larger than those

Table 3
The truncated steady-state equations used in the two-step computations of Fig. 3.

$$C_H\left(k_{1f}C_{O_2}+k_{3b}C_{H_2O}+k_{4f}C_{O_2}C_{M_4}+k_{5f}C_{HO_2}+k_{6f}C_{HO_2}+k_{16f}C_{NH_2}+k_{22b}C_{NH_2}C_{M_{22}}+k_{23f}C_{NH_3}\right)=$$
$$k_{2f}C_{H_2}C_O+k_{3f}C_{H_2}C_{OH}+k_{16b}C_{NH}C_{H_2}+k_{22f}C_{NH_3}C_{M_{22}}+k_{23b}C_{NH_2}C_{H_2}+k_{28b}C_{HNO}C_{M_{28}}$$

$$C_{OH}=\frac{(b^2-4ac)^{1/2}-b}{2a}\quad\text{with}$$

$$a=\frac{k_{19f}k_{25f}C_{NH_3}}{C_H(k_{16f}+k_{22b}C_{M_{22}})+k_{18f}C_{O_2}+k_{23b}C_{H_2}+k_{25b}C_{H_2O}-\frac{k_{18f}k_{24f}C_{O_2}C_{NH_3}}{k_{2f}C_{H_2}+k_{24f}C_{NH_3}}},$$

$$b=k_{2b}C_H+k_{3f}C_{H_2}+k_{7f}C_{HO_2}+k_{8f}C_HC_{M_8}+k_{25f}C_{NH_3}+$$
$$\frac{k_{19f}C_{NH_3}\left(k_{22f}C_{M_{22}}+k_{23f}C_H+\frac{k_{1f}k_{24f}C_HC_{O_2}}{k_{2f}C_{H_2}+k_{24f}C_{NH_3}}\right)-k_{25f}C_{NH_3}(k_{25b}C_{H_2O}+k_{18f}C_{O_2})}{C_H(k_{16f}+k_{22b}C_{M_{22}})+k_{18f}C_{O_2}+k_{23b}C_{H_2}+k_{25b}C_{H_2O}-\frac{k_{18f}k_{24f}C_{O_2}C_{NH_3}}{k_{2f}C_{H_2}+k_{24f}C_{NH_3}}},$$

$$c=-2k_{1f}C_HC_{O_2}-k_{3b}C_{H_2O}C_H-k_{4f}C_HC_{O_2}C_{M_4}-C_{HO_2}(k_{12f}C_{H_2}+C_H(k_{5f}-k_{6f}))-$$
$$\frac{C_{NH_3}(k_{25b}C_{H_2O}+k_{18f}C_{O_2})\left(k_{22f}C_{M_{22}}+k_{23f}C_H+\frac{k_{1f}k_{24f}C_HC_{O_2}}{k_{2f}C_{H_2}+k_{24f}C_{NH_3}}\right)}{C_H(k_{16f}+k_{22b}C_{M_{22}})+k_{18f}C_{O_2}+k_{23b}C_{H_2}+k_{25b}C_{H_2O}-\frac{k_{18f}k_{24f}C_{O_2}C_{NH_3}}{k_{2f}C_{H_2}+k_{24f}C_{NH_3}}}$$

$$C_{NH_2}=\frac{C_{NH_3}\left(k_{22f}C_{M_{22}}+k_{23f}C_H+\frac{k_{1f}k_{24f}C_HC_{O2}}{k_{2f}C_{H_2}+k_{24f}C_{NH_3}}+k_{25f}C_{OH}\right)}{\left[C_H(k_{16f}+k_{22b}C_{M_{22}})+k_{18f}C_{O_2}+k_{23b}C_{H_2}+k_{25b}C_{H_2O}\right]-\frac{k_{18f}k_{24f}C_{O_2}C_{NH_3}}{k_{2f}C_{H_2}+k_{24f}C_{NH_3}}}$$

$$C_{HO_2}=\frac{1}{4k_{11f}}\left\{-C_H(k_{5f}+k_{6f})-k_{12f}C_{H_2}+\left[(C_H(k_{5f}+k_{6f})+k_{12f}C_{H_2})^2+8k_{4f}k_{11f}C_HC_{O_2}C_{M_4}\right]^{1/2}\right\}$$

$$C_{H_2O_2}=\frac{k_{11f}C_{HO_2}^2+k_{12f}C_{HO_2}C_{H_2}}{k_{10f}C_{M_{10}}},\quad C_O=\frac{k_{1f}C_HC_{O_2}+k_{18f}C_{NH_2}C_{O_2}}{k_{2f}C_{H_2}+k_{24f}C_{NH_3}}$$

$$C_{NO}=\frac{k_{14f}C_{O2}(k_{16f}C_H+k_{19f}C_{OH})}{(k_{20f}+k_{21f})(k_{13f}C_{OH}+k_{14f}C_{O_2}+k_{16b}C_{H_2})}+\frac{k_{18f}C_{O_2}}{k_{20f}+k_{21f}}$$

$$C_{HNO}=\frac{C_{NH_2}}{k_{28b}C_{M_{28}}}\left(\frac{k_{14f}C_{O_2}(k_{16f}C_H+k_{19f}C_{OH})}{k_{13f}C_{OH}+k_{14f}C_{O_2}+k_{16b}C_{H_2}}+k_{18f}C_{O_2}\right)$$

$$C_{NH}=\frac{C_{NH_2}(k_{16f}C_H+k_{19f}C_{OH})}{k_{13f}C_{OH}+k_{14f}C_{O_2}+k_{16b}C_{H_2}},\quad C_{N_2H}=\frac{k_{21f}C_{NH_2}C_{NO}}{k_{26f}C_{O_2}+k_{27f}C_{M_{27}}},\quad C_{H_2NO}=\frac{k_{18f}C_{NH_2}C_{O_2}}{k_{31f}C_{HO_2}}$$

obtained with the short mechanism from which it is derived, although the resulting overpredictions, comparable to those found in strained hydrogen flames [24], are acceptable for most computational purposes.

5. Truncated steady-state expressions

Further simplification to the reduced mechanism follows from introducing truncations to the steady-state expressions [23]. The procedure involves the selective removal of elementary reactions that do not change significantly the solution to the nonlinear algebraic equations of Table 2, leading to a simpler system that requires shorter computational times. While reaction 6b was found in the present computations to be entirely unimportant for flame propagation under all conditions, consistent with previous results [12], other truncations depend on the specific combustion conditions considered. For the example presented below, the focus was on conditions that result in burning rates that are not too dissimilar from those of natural-gas/air mixtures, of interest for retrofitting of natural-gas turbines. Substantial truncations were applied in this case to greatly simplify the expressions while maintaining reasonable burning velocities. The reactions needed for the description of combustion under those conditions are written in bold font in Table 2.

The truncation procedure continued by using algebraic manipulation to further simplify the solution. Although explicit expressions for the different radical concentrations as a function of the reactants and products concentrations and temperature could not be found, the set of truncated steady-state equations, given in Table 3, is organized in a way that effectively reduces the problem to the solution of a single non-linear equation. The development is based on the observation that all intermediates can be expressed as explicit functions of C_H. For example, the OH concentration can be obtained as a function of C_H by substituting the expressions for C_{HO_2} into the expressions for the coefficients b and c that appear in the steady-state expression for C_{OH}. Similarly, the concentration of NH_2 appearing in Table 3 can be written in terms of C_H by expressing C_{OH} as a function of C_H. These explicit expressions can be used in the steady-state equation for H (the top entry in Table 3) to generate a single non-linear equation for C_H that can be trivially solved computationally for given values of T, C_{O_2}, C_{H_2}, C_{NH_3}, C_{H_2O}, and C_{N_2}. Once C_H is known, the result can be substituted into the remaining explicit equations to obtain the concentration of the other intermediates.

The truncated expressions in Table 3 were used in the computations of laminar-flame propagation velocities shown by the dot-dashed curves in Fig. 3. As can be seen, the accordance with the detailed and short chemistry results is reasonably good, departures remaining smaller than 20% under all conditions explored in the figure. The results indicate that the truncated two-step mechanism can provide sufficient accuracy for describing oxidation of certain ammonia-hydrogen blends at high pressure while significantly reducing computational times.

6. Discussion and conclusions

Starting with a recently derived 60-step mechanism [5], reduced-chemistry descriptions have been developed for combustion of ammonia-hydrogen blends at conditions of pressure, temperature and

dilution typically found in gas-turbine combustors. A short mechanism involving only 16 reactive species and 31 elementary reactions, 10 of them being reversible, has been shown to predict ignition delay times and burning rates with accuracy comparable to those of much larger mechanisms. Furthermore, because of the existing high pressure placing the system not far from the crossover temperature of hydrogen-oxygen combustion, in deflagrations all intermediates are shown to follow a good steady-state approximation, enabling the derivation of a reduced mechanism in which the oxidation process is described by two overall reactions featuring O_2, H_2, and NH_3 as reactants and N_2 and H_2O as combustion products. The evaluation of the associated global rates, involving a number of elementary reactions, requires the solution of the nonlinear algebraic equations resulting from the production-reaction balances of the 11 steady-state species. The two-step reduced description, and the simplified version obtained after truncation of the steady-state expressions, are tested through computations of burning rates of preheated mixtures at high pressure.

The accuracy achieved by the reduced descriptions developed here is likely to be sufficient for use in many investigations based on computational fluid dynamics, thereby facilitating modeling efforts for guiding designs of robust, reliable, and safe gas-turbine combustors employing ammonia-hydrogen blends. To investigate the ability of the reduced mechanisms to describe flow-chemistry interactions, future computational tests should consider nonpremixed strained flamelets as well as partially premixed conditions. Steady-state approximations, which have been shown here to apply with reasonable accuracy to the description of freely propagating flames, might be applicable for some intermediates during autoignition processes, thereby motivating further investigations of reduced mechanisms containing more than two overall reactions.

CRediT authorship contribution statement

Brandon Li: Writing – review & editing, Writing – original draft, Methodology, Investigation, Formal analysis, Data curation. **Daniel Fernández-Galisteo:** Writing – review & editing, Software, Investigation, Formal analysis. **Antonio L. Sánchez:** Writing – review & editing, Writing – original draft, Supervision, Project administration, Formal analysis, Conceptualization. **Forman A. Williams:** Writing – review & editing, Writing – original draft, Supervision, Project administration, Formal analysis, Conceptualization.

Declaration of competing interest

The authors declare that they have no known competing financial interests or personal relationships that could have appeared to influence the work reported in this paper.

References

[1] A. Dreizler, H. Pitsch, V. Scherer, C. Schultz, J. Janicka, The role of combustion science and technology in low and zero impact energy transformation processes, Appl. Energy Combust. Sci. 7 (2021) 100040.
[2] D. Burnes, P. Saxena, R. Kurz, Study to adapt industrial gas turbines for significant and viable CO_2 emissions reduction, J. Eng. Gas Turbines Power 145 (2023) 011021.
[3] M.R. Bothien, A. Ciani, J.P. Wood, F. G., Toward decarbonized power generation with gas turbines by using sequential combustion for burning hydrogen, J. Eng. Gas Turbines Power 141 (2019) 121013.
[4] M. Reith, A. Gruber, F.A. Williams, J.H. Chen, Enhanced burning rates in hydrogen-enriched turbulent premixed flames by diffusion of molecular and atomic hydrogen, Combust. Flame 239 (2022) 111740.
[5] Y. Jiang, A. Gruber, K. Seshadri, F. Williams, An updated short chemical-kinetic nitrogen mechanism for carbon-free combustion applications, Int. J. Energy Res. 44 (2020) 795–810.
[6] H. Xiao, A. Valera-Medina, P.J. Bowen, Modeling combustion of ammonia/hydrogen fuel blends under gas turbine conditions, Energy Fuels 31 (2017) 8631–8642.
[7] J. Otomo, M. Koshi, T. Mitsumori, H. Iwasaki, K. Yamada, Chemical kinetic modeling of ammonia oxidation with improved reaction mechanism for ammonia/air and ammonia/hydrogen/air combustion, Int. J. Hydrog. Energy 43 (2018) 3004–3014.
[8] H. Kobayashi, A. Hayakawa, K.K.A. Somarathne, E.C. Okafor, Science and technology of ammonia combustion, Proc. Combust. Inst. 37 (2019) 109–133.
[9] W.S. Chai, Y. Bao, P. Jin, G. Tang, L. Zhou, A review on ammonia, ammonia-hydrogen and ammonia-methane fuels, Renew. Sustain. Energy Rev. 147 (2021) 111254.
[10] D. Greenblatt, L. Tian, R. Lindstedt, The impact of hydrogen substitution by ammonia on low-and high-temperature combustion, Combust. Flame (2023) 112733.
[11] R.P. Lindstedt, M.A. Selim, Reduced reaction mechanisms for ammonia oxidation in premixed laminar flames, Combust. Sci. Technol. 99 (1994) 277–298.
[12] A.L. Sánchez, F.A. Williams, Recent advances in understanding of flammability characteristics of hydrogen, Prog. Energy Combust. Sci. 41 (2014) 1–55.
[13] The San Diego mechanism: Chemical-kinetic mechanisms for combustion applications, 2016, Version: 2018-07-23.
[14] R.J. Kee, G. Dixon-Lewis, J. Warnatz, M.E. Coltrin, J.A. Miller, A Fortran Computer Code Package for the Evaluation of Gas-Phase Multicomponent Transport Properties, Tech. Rep. SAND86-8246, Sandia Labs., Livermore, CA (United States), 1986.
[15] P.H. Paul, DRFM: A New Package for the Evaluation of Gas-Phase Transport Properties, Tech. Rep., Sandia Labs., Livermore, CA (United States), 1997.
[16] A. Ichikawa, A. Hayakawa, Y. Kitagawa, K. Kunkuma Amila Somarathne, T. Kudo, H. Kobayashi, Laminar burning velocity and markstein length of ammonia/hydrogen/air premixed flames at elevated pressures, Int. J. Hydrog. Energy 40 (2015) 9570–9578.
[17] B. Jin, Y. Deng, G.-x.L. Li, H.-m. Li, Experimental and numerical study of the laminar burning velocity of NH_3/H_2/air premixed flames at elevated pressure and temperature, Int. J. Hydrog. Energy 47 (2022) 36046–36057.
[18] M. Pochet, V. Dias, B. Moreau, F. Foucher, H. Jeanmart, F. Contino, Experimental and numerical study, under LTC conditions, of ammonia ignition delay with and without hydrogen addition, Proc. Combust. Inst. 37 (2019) 621–629.
[19] G.D. Alamo, F.A. Williams, A.L. Sánchez, Hydrogen–oxygen induction times above crossover temperatures, Combust. Sci. Technol. 176 (2004) 1599–1626.
[20] J. Zhang, B. Mei, W. Li, J. Fang, Y. Zhang, C. Cao, Y. Li, Unraveling pressure effects in laminar flame propagation of ammonia: A comparative study with hydrogen, methane, and ammonia/hydrogen, Energy Fuels 36 (2022) 8528–8537.
[21] P.A. Libby, A. Liñán, F.A. Williams, Strained premixed laminar flames with nonunity Lewis numbers, Combust. Sci. Technol. 34 (1–6) (1983) 257–293.
[22] F.A. Williams, Combustion Theory, second ed., CRC Press, 2018.
[23] N. Peters, B. Rogg, Reduced Kinetic Mechanisms for Applications in Combustion Systems, Springer-Verlag, Heidelberg, 1993.
[24] J. Carpio, B. Li, D. Fernández-Galisteo, A.L. Sánchez, F.A. Williams, Systematically derived one-step kinetics for hydrogen-air gas-turbine combustion, Combust. Flame 250 (2023) 112633.